Effects of spin-orbit coupling in superconducting proximity devices: Application to CoSi$_2$/TiSi$_2$ heterostructures

Vivek Mishra [1], Yu Li,[1] Fu-Chun Zhang,[1,2,3,*] and Stefan Kirchner [4,5,†]

[1]*Kavli Institute for Theoretical Sciences, University of Chinese Academy of Sciences, Beijing 100190, China*
[2]*CAS Center for Excellence in Topological Quantum Computation, University of Chinese Academy of Sciences, Beijing 100190, China*
[3]*Collaborative Innovation Center of Advanced Microstructures, Nanjing University, Nanjing 210093, China*
[4]*Zhejiang Institute of Modern Physics and Department of Physics, Zhejiang University, Hangzhou 310027, China*
[5]*Zhejiang Province Key Laboratory of Quantum Technology and Device, Zhejiang University, Hangzhou 310027, China*

Motivated by the recent findings of unconventional superconductivity in CoSi$_2$/TiSi$_2$ heterostructures, we study the effect of interface-induced Rashba spin-orbit coupling on the conductance of a three-terminal T-shaped superconducting device. We calculate the differential conductance for this device within the quasiclassical formalism that includes the mixing of triplet-singlet pairing due to the Rashba spin-orbit coupling. We discuss our result in light of the conductance spectra reported by S.-P. Chiu *et al.*, arXiv:2012.13679 for CoSi$_2$/TiSi$_2$ heterostructures.

I. INTRODUCTION

The search for platforms that can host Majorana zero modes (MZMs) has been one of the major topics driving current condensed-matter research because MZMs, being localized quasiparticles that obey non-Abelian braiding statistics, are the essential ingredient for topological quantum computing [1–6]. Early proposals for creating MZMs involve spin triplet superconductivity, while almost all known superconductors belong to the spin singlet class with a few possible exceptions such as UPt$_3$. As a result, a variety of ingenious heterostructures of superconducting nanowires have been proposed and observed to generate the required *p*-wave pairing component, taking advantage of broken time-reversal and inversion symmetries [7–10]. MZMs have also been proposed inside a vortex of a topological superconductor [11]; the experimental observation of a MZM in some iron-based superconductors is along this line [12,13]. Fu and Kane [14] proposed that the proximity of the *s*-wave superconductor on the surface of a three-dimensional topological insulator may serve the same purpose to generate MZMs due to the spin-momentum locking. Their proposal has been confirmed experimentally [15].

To distinguish between singlet and triplet superconductors, in addition to nuclear magnetic resonance [16] and muon spin rotation (μSR) probe, a T-shaped proximity structure junction was proposed to probe the presence of triplet superconductivity [17]. The proposed device consists of two normal metal wires combined to form the letter T. This three-terminal device is connected to a superconductor at the free end of the leg (see Fig. 1). As shown in Ref. [17], a chiral *p*-wave or

an ordinary *p*-wave state gives a zero-bias conductance peak (ZBCP) in response to bias voltage between the open ends of the bar of the T.

Recent experimental results reported by Chiu *et al.* have been argued to be consistent with the occurrence of chiral *p*-wave pairing in CoSi$_2$/TiSi$_2$ heterostructures [18]. Chiu *et al.* support their claim with conductance spectroscopy data for CoSi$_2$/TiSi$_2$ superconductor-normal-metal (SN) tunnel junctions. In these heterostructures, CoSi$_2$ is the superconducting component which becomes superconducting below 1.5 K. The conductivity of the SN tunnel junctions agrees with the theoretical calculations based on the Blonder-Tinkham-Klapwijk (BTK) model for a chiral *p*-wave superconductor [19]. However, there is a sharp zero-bias peak in the conductance spectra of the SN junction which cannot be described within the BTK theory.

Chiu *et al.* further substantiated their interpretation with conductance spectra based on three-terminal T-shaped proximity devices similar to the one sketched in Fig. 1, which again show ZBCPs. As noted in Ref. [18], a distinction between ordinary and chiral *p*-wave superconductors based on solely experimental conductance spectra is hardly feasible. The observation of hysteresis behavior in the magnetoresistance below the superconducting transition temperature T_c of the CoSi$_2$/TiSi$_2$ junctions, however, further vindicates their claim of chiral *p*-wave in the CoSi$_2$/TiSi$_2$ heterostructures. The findings of Ref. [18] are intriguing for a few reasons. The superconductivity in CoSi$_2$ was discovered in 1952 [20]; the theoretical estimate of T_c based on phonon-mediated pairing appears to agree well with the experimental T_c [21]. The specific heat data below the superconducting state suggest conventional *s*-wave pairing [22]. This material does not appear to be located in the vicinity of magnetism; therefore, there is no reason to expect it to be a chiral *p*-wave superconductor, at least in the bulk limit.

*fuchun@ucas.ac.cn
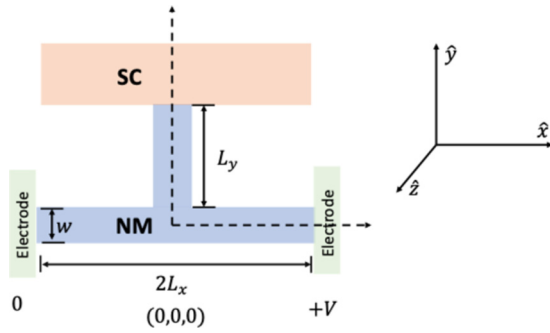†stefan.kirchner@correlated-matter.com

FIG. 1. Schematic illustration of a T-shaped junction. The three-terminal proximity device consists of a diffusive normal metal (NM) part attached to a superconductor (SC). The blue area indicates the diffusive normal metal (NM) part of the device, while the orange area shows the SC part.

It is worth noting that a strong spin-orbit coupling (SOC), exceeding the superconducting gap of $CoSi_2$ by more than a factor 30, was reported in $CoSi_2$ by the same group [18]. Having in mind this strong SOC, we propose the substrate-induced Rashba SOC as a source of p-wave pairing in this system. It is known that SOC-induced pairing does not break the time-reversal symmetry [23], and the presence of the SOC also leads to mixing of the triplet and singlet components. In the context of noncentrosymmetric superconductors, the tunneling conductance for SN junctions has been studied in systems with SOC [24–28]. However, the effect of the SOC and the conductance for a mixed-parity superconductor in a T-junction device is not known. The original T-junction study did not include the SOC, and the ZBCP for a chiral p-wave superconductor is expected to be weak [17].

In this paper, we investigate the effect of the singlet-triplet mixing on the conductance spectra of the T-shaped junctions. In the context of $CoSi_2/TiSi_2$ heterostructures, we focus on substrate-induced SOC in a superconductor, which results in the "sp" pairing state, where the singlet component has s-wave symmetry and the triplet component has p-wave symmetry. In principle, triplet and singlet components can have anisotropic structures due to the orbital form factors and because the bands crossing the Fermi energy derive from the $3d$ orbitals of Co [21]. Thus, we also consider the "df" and "dp" pairing states, which have additional orbital form factors compatible with $d_{x^2-y^2}$ and d_{xy} functions, which lead to $d_{x^2-y^2}$ and d_{xy} structures for the singlet components and effectively f-wave- and p-wave-like structures for the triplet components, respectively. The df state was proposed for a few heavy-electron noncentrosymmetric systems [29,30], and the dp state was suggested for $LaAlO_3/SrTiO_3$ heterointerfaces [26].

II. MODEL AND FORMALISM

We model the $CoSi_2/TiSi_2$ T-shaped junction of Ref. [18] in terms of the two-dimensional proximity devices depicted schematically in Fig. 1. The transport in the normal metal (NM) part is assumed to be diffusive and is the experimentally relevant regime. The height d and the width w are very small compared to its length $L_{x/y}$ in either direction, and its dimensions are assumed to be very small compared to

the coherence length $\xi_0 \equiv \hbar v_F/\pi \Delta$ (i.e., $w, d \ll \xi_0$), where v_F and Δ are the Fermi velocity and the superconductivity gap, respectively. Within the ambit of these assumptions, this structure can be thought of as a set of two one-dimensional wires joined to form the shape of the letter T. The leg of this T-shaped junction is attached to a clean superconductor. The ends of the horizontal section of this junction are subjected to a bias voltage eV. We consider the case where the SOC exists in the superconducting component of this structure due to its broken inversion symmetry.

The kinetic part of the Hamiltonian reads

$$H_{\mathbf{k}} = \xi_{\mathbf{k}} + H_{SOC,\mathbf{k}}. \tag{1}$$

Here $\xi_{\mathbf{k}}$ is the electronic dispersion relation for the fermions, and the SOC term is

$$H_{SOC,\mathbf{k}} = \alpha(\boldsymbol{\sigma} \times \mathbf{k}) \cdot \hat{z} = \alpha \mathcal{A}_{\mathbf{k}} \cdot \boldsymbol{\sigma}, \tag{2}$$

where α is the Rashba SOC coupling constant and $\boldsymbol{\sigma}$ is $(\sigma_x, \sigma_y, \sigma_z)$, where $\sigma_{x/y/z}$ are the Pauli matrices in spin space. We consider the Rashba SOC that is induced along the growth direction, which is chosen to be the $\hat{z}$ direction in the T-shaped junction. In this case, the normal to the relevant interface is along the $\hat{z}$ axis, and the SOC vector is

$$\mathcal{A}_{\mathbf{k}} = (k_y, -k_x, 0) = |k|(\sin\phi_k, -\cos\phi_k, 0), \tag{3}$$

where ϕ_k is the angle in the two-dimensional momentum space.

Diagonalizing the Hamiltonian results in a splitting of the original band into two helical bands with different spin structures. The energies of these two bands are $\xi_{\mathbf{k}} \pm \alpha|\mathbf{k}|$. The changes in the density of states and the Fermi velocities are of the order of $\alpha p_F/E_F$, where p_F and E_F are the Fermi momentum and the Fermi energy of the original band. For realistic systems, the SOC energy is generally very small compared to the Fermi energy. Therefore, we ignore these differences in the density of states and the Fermi velocities between the helical bands, and we take these parameters to be the same as the original band for our subsequent calculations.

We assume that the superconducting component is confined in the two-dimensional plane and that it has dimensions that are very large compared to the coherence length; hence, we treat it like a homogeneous system and ignore any kind of inverse proximity effect due to the junction formation. We adopt the quasiclassical Keldysh formalism to carry out the conductance calculations [31], where the quasiclassical Green's function consists of retarded, advanced, and Keldysh components. Each of these components is a 4×4 matrix in the Nambu-spin space. We denote the 4×4 Green's function in this space by $\check{}$, and $\hat{}$ denotes the 2×2 Green's functions in the spin basis. The advanced and Keldysh components can be obtained from the retarded component, on which we focus in the following. Following Ref. [32], the quasiclassical retarded Green's function in a superconductor without inversion symmetry can be expressed as

$$\check{g} = \begin{pmatrix} g_I\sigma_I + g_{II}\sigma_{II} & (f_I\sigma_I + f_{II}\sigma_{II})i\sigma_y \\ -i\sigma_y(\bar{f}_I\sigma_I + \bar{f}_{II}\sigma_{II}) & \sigma_y(\bar{g}_I\sigma_I + \bar{g}_{II}\sigma_{II})\sigma_y \end{pmatrix}, \tag{4}$$

where $\quad \sigma_{I/II} = (\sigma_0 \pm \mathcal{A}_\mathbf{k} \cdot \boldsymbol{\sigma})/2, \quad g_{I/II}(\varepsilon) = \varepsilon/\sqrt{\varepsilon^2 - \Delta^2_{I/II}}$, $f_{I/II}(\varepsilon) = \Delta_{I/II}/\sqrt{\varepsilon^2 - \Delta^2_{I/II}}$, $\bar{g}_{I/II} = -g_{I/II}$, and $\bar{f}_{I/II} = f_{I/II}$. The general gap structure for a system with the SOC is [33]

$$\hat{\Delta} = [\Delta_s \Phi_s(\phi_k) + \Delta_t \Phi_t(\phi_k) \mathcal{A}_\mathbf{k} \cdot \boldsymbol{\sigma}] i\sigma_y. \tag{5}$$

Here the SOC vector $\mathcal{A}_\mathbf{k}$ acts like the **d** vector, and Δ_s (Δ_t) is the gap magnitude of the singlet (triplet) component. Since SOC energy is very large compared to T_c in any realistic material, we ignore any kind of interband pairing between the helical bands [34]. The gaps on two helical bands are $\Delta_{I/II} = \Delta_s \Phi_s \pm \Delta_t \Phi_t$. The angular anisotropy of the gaps is embedded in Φ_s and Φ_t. The simplest case is $\Phi_s = \Phi_t = 1$, which is referred to as the *sp* state, where the singlet component is an isotropic *s*-wave state and the triplet component has *p*-wave structure. Such states have been proposed for various noncentrosymmetric superconductors; self-consistent model calculations have found stable ground states with singlet- or triplet-dominant components depending on the strength of pairing in the respective channels [33]. Here we use $\Delta_{s/t}$ as parameters in our calculations. Apart from this, the other possibilities are the *df* state, where $\Phi_s = \Phi_t = \cos 2\phi_k$, and the *dp* state, with $\Phi_s = \Phi_t = \sin 2\phi_k$. We focus on the *sp* state, which is more relevant in the context of CoSi$_2$/TiSi$_2$ heterostructures. The gap function is parameterized as

$$\hat{\Delta} = \Delta_0 \left(\frac{1}{\sqrt{1+r^2}} + \frac{r}{\sqrt{1+r^2}} \mathcal{A}_\mathbf{k} \cdot \boldsymbol{\sigma} \right) i\sigma_y, \tag{6}$$

where Δ_0 is $\sqrt{\Delta_s^2 + \Delta_t^2}$ [35]. Here the parameter $r \in [0, \infty)$ is the ratio of the triplet component to the singlet component.

The Cooper pairs from the superconducting side can tunnel into the diffusive NM, and this effect is included through the boundary conditions, which are used to solve the Usadel equations on the NM side. We treat the barrier between the NM and the superconductor as a spin-independent barrier. This assumption is justified because the SOC is very small compared to the Fermi energy [27]. We first calculate the retarded component of the quasiclassical Green's function $\check{g}_n^R$ and then construct the advanced and Keldysh components using $\check{g}_n^R$. The subscript n denotes the normal metal. The Usadel equations for $\check{g}_n^R$ are

$$D\partial_\ell(\check{g}_n^R \partial_\ell \check{g}_n^R) + i[\varepsilon\check{\tau}_3, \check{g}_n^R] = 0, \tag{7}$$

where D is the diffusion constant of the normal metal, ℓ denotes the spatial direction x or y, and $\check{\tau}_3$ is diag$(1, 1, -1, -1)$. The normalization condition for the quasiclassical Green's function is $\check{g}_n^R \check{g}_n^R = \check{\mathbf{1}}$. These equations are supplemented by the boundary conditions: $\check{g}_n^R = \check{\tau}_3$ at the diffusive metal and electrode interface $(\pm L_x, 0)$, and $\check{g}_n^R \partial_y \check{g}_n^R = \check{0}$ at the crossing point $(0,0)$, where the last condition reflects current conservation [36]. The boundary condition at $(0, L_y)$ depends on the nature of the gap in the superconductor. We use the boundary condition derived by Nazarov for interfaces with arbitrary transparency [37], which was generalized for unconventional superconductors by Tanaka *et al.* [38–42]. In this approach, the interface is modeled as a δ function potential barrier

$H\delta(y - L_y)$, which has the transmission probability

$$T(\phi) = \frac{4\cos^2 \phi}{4\cos^2 \phi + Z^2}, \tag{8}$$

where ϕ is the angle measured with respect to the normal to the interface, which is the y axis in the geometry we consider, and Z is a dimensionless parameter given by $Z = 2mH/k_F^2$. Here m is the effective mass, and k_F is the Fermi momentum. A large value of Z gives an interface with poor transparency, whereas $Z = 0$ characterizes a transparent interface. The boundary condition at the SN interface can be expressed as

$$L_y \check{g}_n \frac{\partial \check{g}_n}{\partial y} \bigg|_{y=L_y} = 2\Gamma \langle [\check{g}_n, \check{B}(\phi)] \rangle_\phi, \tag{9}$$

where $\check{g}_n$ on the right-hand side of Eq. (9) is the quasiclassical Green's function in the NM region evaluated at $(0, L_y)$ and Γ is the ratio of the normal metal resistance R_N and the interface resistance R_B. The angular average on the right-hand side of Eq. (9) is defined as

$$\langle \cdots \rangle_\phi = \frac{\int_{-\pi/2}^{\pi/2} d\phi (\cdots) \cos \phi}{\int_{-\pi/2}^{\pi/2} d\phi T(\phi) \cos \phi}. \tag{10}$$

Note that the angle ϕ in the boundary condition is measured with respect to the interface normal. The matrix function $\check{B}$ in Eq. (9) is

$$\check{B}(\phi) = (-T'[\check{g}_n, \check{H}_-^{-1}] + \check{H}_-^{-1}\check{H}_+ - T'^2\check{g}_n\check{H}_-^{-1}\check{H}_+)^{-1}$$
$$\times [-T'(\check{\mathbf{I}} + \check{H}_-^{-1}) + T'^2\check{g}_n\check{H}_-^{-1}\check{H}_+], \tag{11}$$

$$T'(\phi) = \frac{T(\phi)}{2 - T(\phi) + 2\sqrt{1 - T(\phi)}}, \tag{12}$$

$$\check{H}_\pm = \frac{1}{2}[\check{g}(\phi) \pm \check{g}(\pi - \phi)]. \tag{13}$$

Note that the boundary condition itself depends on the solution at the boundary. To calculate the differential conductance, we first calculate the current. For the current calculation, we need the Keldysh component of the quasiclassical Green's function,

$$\check{g}^K = \check{g}^R \check{h} - \check{h}\check{g}^A, \tag{14}$$

where the advanced component is

$$\check{g}^A = -\check{\tau}_3(\check{g}^R)^\dagger \check{\tau}_3 \tag{15}$$

and the spin-resolved distribution function $\check{h}$ is a diagonal matrix diag$(f_{L\uparrow} + f_{T\uparrow}, f_{L\downarrow} + f_{T\downarrow}, f_{L\uparrow} - f_{T\uparrow}, f_{L\downarrow} - f_{T\downarrow})$ [43], where $f_{T\nu}$ and $f_{L\nu}$ are the transverse and longitudinal distribution functions and ν is the spin index. In the T-shaped junction, a bias voltage V is applied at $x = +L_x$, and at the other end the voltage is kept at zero. Therefore, the equilibrium spin-resolved distribution functions at these two ends are

$$f_{T\uparrow/\downarrow}\bigg|_{x=L_x, y=0} = \frac{1}{2}\left[n_f\left(\frac{\varepsilon_-}{2T}\right) - n_f\left(\frac{\varepsilon_+}{2T}\right)\right], \tag{16}$$

$$f_{T\uparrow/\downarrow}\bigg|_{x=-L_x, y=0} = 0. \tag{17}$$

Here n_f is the Fermi-Dirac distribution function, and $\varepsilon_\pm = \varepsilon \pm eV$. The transverse component of the distribution function
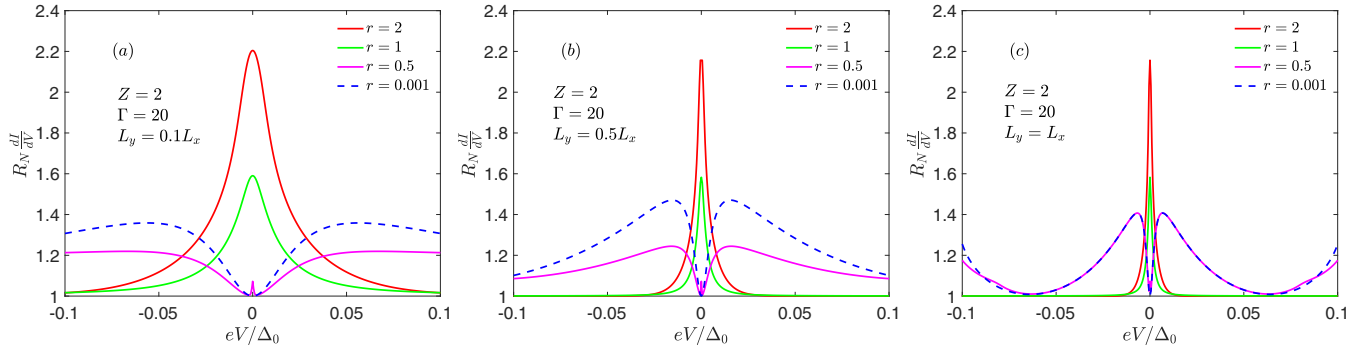
FIG. 2. Differential conductance for a T-shaped junction attached to a superconductor under the influence of Rashba SOC. The parameter r is the ratio of the triplet component to singlet component of the order parameter. The interface quality parameter Γ is set to 20. The ratio of lengths along the two spatial directions L_y/L_x is 0.1, 0.5, and 1 in (a), (b), and (c), respectively. The differential conductance is calculated in the zero-temperature limit.

will be the same for both spin components at the normal electrode. The charge current density is

$$J_E(x, T) = \frac{eN_0 D}{8} \int_{-\infty}^{\infty} d\varepsilon \text{Tr}\big[\hat{\tau}_3 (\check{g}^R \partial_x \check{g}^K + \check{g}^K \partial_x \check{g}^A)\big]. \quad (18)$$

Here N_0 is the total density of states at the Fermi level. The differential conductance can be obtained by evaluating the derivative of the charge current density with respect to the bias voltage; we numerically solve the Usadel equations in the normal metal and with the aforementioned boundary conditions. Since the boundary condition at the SN interface involves the solutions at the interface, we start with a guess solution and obtain the final solution using the fixed-point iteration method.

III. RESULTS AND DISCUSSION

We consider a good interface between NM and SC and fix Γ at a value of 20. The interface barrier parameter Z is set to 2. A larger value of Γ represents a good-quality surface, which is essential for the formation of a sizable proximity effect. Figure 2 shows the differential conductance for the T-shaped device, where the superconducting portion is under the influence of the substrate-induced Rashba SOC for several values of the parameter r, indicating the relative strength of the triplet component. The magnitude of the gap is $0.05E_{th}$, where E_{th} is the Thouless energy for the half wire along the $\hat{x}$ direction, i.e., $E_{th} \equiv \hbar D/L_x^2$. For the proximity problem, the characteristic energy scale in the NM is the Thouless energy, which is inversely proportional to the square of the device length. A smaller device is usually better for observing proximity effect related physics.

For large values of r, the triplet component dominates. In this regime we find that the differential conductance is similar to that in the p-wave case [17]. In general, for a three-dimensional system, a $\hat{z}$ Rashba SOC gives $\Delta_s \pm \Delta_t \sin\theta$, where θ is the polar angle. Therefore, a triplet-dominated system will have horizontal line nodes. However, in our study we consider a two-dimensional system where the gaps on the two helical bands are $\Delta_s \pm \Delta_t$. Thus, in the triplet-dominant limit ($r > 1$), we have isotropic unequal gaps on two bands with opposite chiralities. A ZBCP is expected for a chiral p-wave superconductor [17]; however, it is expected to be weaker than a p-wave system. We find that the height of the peak is com-

parable to that of a p-wave system. Unlike in chiral p-wave superconductors, the time-reversal symmetry is not broken in the case considered here. The origin of the peak is the symmetry of the induced pairing in the NM. In the diffusive metal, the isotropic s-wave state can survive due to impurity scattering, which kills any other kind of superconducting state. In the superconducting side of the junction, both triplet and singlet components are even functions of frequency. Therefore, the triplet component leaks odd frequency, even parity, and spin triplet pairs, and the odd frequency nature of these induced pairs gives rise to a ZBCP [41,44,45]. In the case of two helical bands with an opposite-chirality triplet state, the spectral weight of the ZBCP is larger than that expected for a chiral superconductor. The ZBCP becomes sharper as the length of the leg L_y attached to the superconductor increases; therefore, a T-shaped junction with a shorter leg provides a better chance of ZBCP detection. We find that a ZBCP forms as long as the triplet component is stronger. For the special case of $r = 1$, for which triplet and singlet components are equal, we still find a ZBCP in the differential conductance, albeit with a reduced height and width. Since one of the bands has a zero gap in this limit, the height of the peak decreases; the origin of the reduced width in the ZBCP for smaller r is the presence of even frequency, the spin singlet, and even-parity pairs, which come from the singlet component in the mixed-parity superconducting state. Such pairs reduce the density of states at the Fermi level, which reduces the conductivity. However, induced pairs also increase conductivity in the diffusive metal; this increase comes through a Maki-Thompson-like process [46]. These two countereffects cancel at zero energy. The finite-energy maximum in the conductivity near the Thouless energy scale arises due to different decay patterns of these two effects. The negative contribution from the loss of density of states decays exponentially, while the Maki-Thompson-like contribution decays nonexponentially over the energy scale of E_{th}. These two opposite contributions result in a dip in the limit of a pure singlet superconductor ($r \ll 1$) in the T-shaped junction. In the singlet-dominated regime ($0 < r < 1$), we find both a dip from the singlet component and a weak ZBCP from the triplet component. Figure 3 shows the evolution of the conductance peak to a dip in the strong-singlet limit. The width and height of the ZBCP decrease rapidly with a diminishing triplet component.
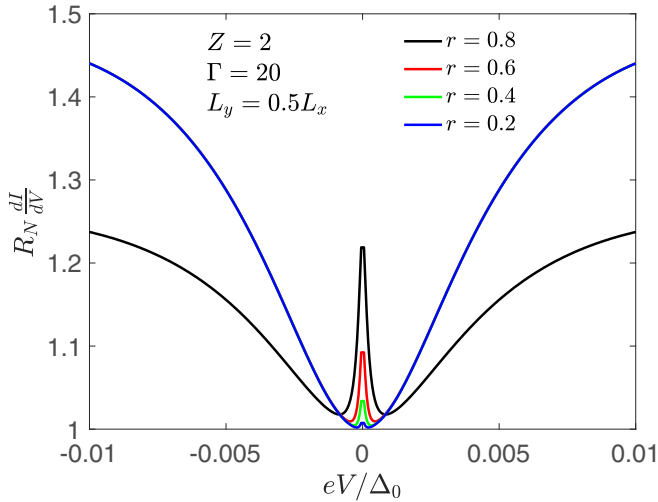
FIG. 3. The differential conductance for a T-shaped junction of a dp superconductor for several values of r with a larger singlet component. The length along the $\hat{y}$ direction is $0.5L_y$.

Next, we consider df and dp states which possess anisotropic orbital components. For the df state, Φ_s and Φ_t are modeled by $\cos 2\phi_k$. For this gap function, there are two line nodes at an angle $\pm\pi/4$ with respect to the interface normal $\hat{y}$ axis. Since we have already shown that a T-shaped junction with shorter leg length is better for observing the ZBCP, we fix the value of L_y at $0.5L_x$ and consider a good quality interface with $\Gamma = 20$ and $Z = 2$ for our differential conductance calculations with anisotropic form factors. Figure 4 shows the differential conductance for a T-shaped junction attached to a df-symmetry superconductor. We find behavior for a df superconductor qualitatively similar to that of the sp superconductor which was discussed above. This qualitative similarity between sp and df superconductors can
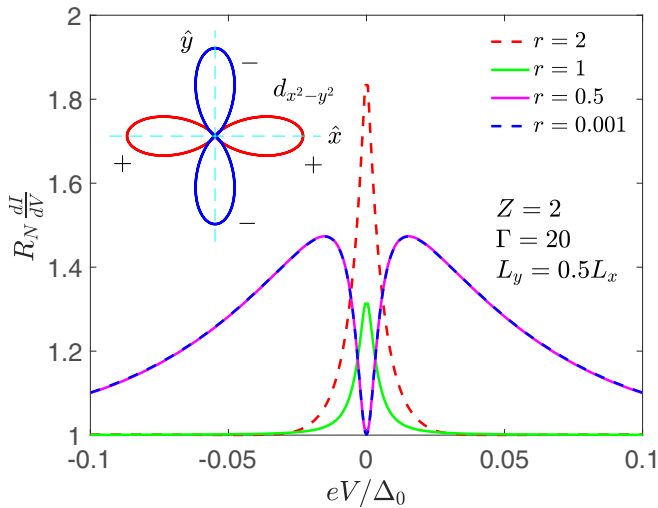

FIG. 4. The differential conductance for a T-shaped junction of a df superconductor for several values of r. The length along the $\hat{y}$ direction is $0.5L_y$. The orientation of the $d_{x^2-y^2}$ orbital form factor is shown in the main plot. The leg of the T junction is taken along the $\hat{y}$ direction, and the voltage is applied along the $\hat{x}$ direction.
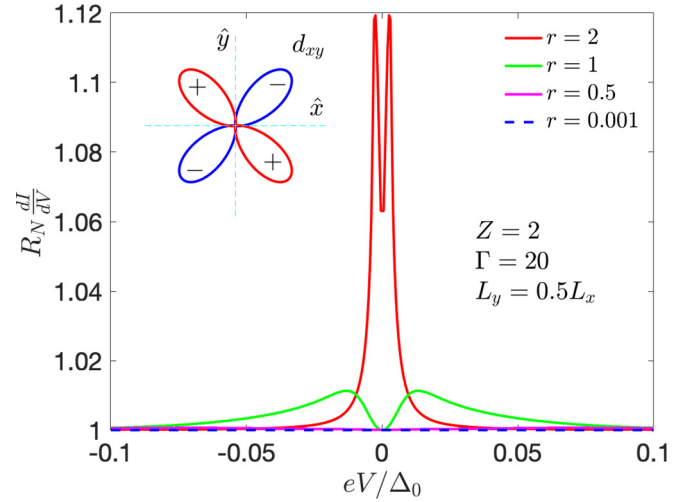

FIG. 5. The differential conductance for a T-shaped junction of a dp superconductor for several values of r. The length along the $\hat{y}$ direction is $0.5L_y$. The orientation of the d_{xy} orbital form factor is shown in the main plot. The leg of the T junction is taken along the $\hat{y}$ direction, and the voltage is applied along the $\hat{x}$ direction.

be understood by examining the phase shift in the gap functions of incoming and outgoing quasiparticle trajectories at the interface. For the $d_{x^2-y^2}$ orbital function, the incoming $\Delta(\phi)$ and the outgoing $\Delta(\pi - \phi)$ are qualitatively the same as the sp superconductor. The nodal line of the $d_{x^2-y^2}$ form factor is at an angle of $\pm\pi/4$, so there is no additional sign change due to this anisotropic factor, and the triplet component is effectively the same as for the sp superconductor. However, the $d_{x^2-y^2}$ form factor reduces the height of the ZBCP in the triplet-dominated regime ($r \geqslant 1$), and in the strong-singlet regime $r < 1$, the tiny peak that we find for the sp superconductors is smeared, and the line shape is similar to an s-wave superconductor.

In contrast, we find a qualitatively different behavior for the dp state; as shown in Fig. 5, there is a splitting of the ZBCP with reduced heights. For a d_{xy} orbital factor, the nodal line is along the interface normal; therefore, for all the incoming gap functions the d_{xy} form factor gives a sign change to the outgoing gap function. The triplet component has an additional chiral p-wave factor, which also gives a sign change between the incoming and outgoing gap functions, which gets canceled by the sign change from the d_{xy} factor; hence, there is no overall sign change. This is qualitatively equivalent to an extended s-wave state. For triplet-dominant cases, a ZBCP with splitting is the outcome of this lack of sign change. In the case of an s-wave superconductor, two opposite contributions to the conductivity exist: while the loss of density of states reduces the conductivity, Maki-Thompson-like processes result in an enhancement. For isotropic s-wave systems, these two effects cancel at zero energy. However, the additional anisotropy from the orbital form factor may not give an exact cancellation, which could lead to an increased conductivity at the zero energy in comparison with a pure isotropic s-wave superconductor. In the limit of a strong-singlet component, we find featureless conductivity. This is expected because the

nodal line is parallel to the interface normal, and in such an orientation no proximity effect occurs [47].

IV. CONCLUDING REMARKS

In this paper, we have studied the conductance of T-shaped junctions connected to a superconductor under the influence of a strong Rashba SOC generated by the underlying substrate. The **d** vector in the superconducting state is determined by the SOC. The superconducting state is a mixed-parity state with both singlet and triplet components. We calculated the tunneling conductance for this system within the quasiclassical formalism. The effect of the superconducting order is included through Nazarov-Tanaka boundary conditions. We looked at the effect of the device size on the zero-bias conductance peak. In agreement with earlier work, we found that smaller device dimensions result in larger full width at half maximum (FWHM) of the ZBCPs. Moreover, we showed that both triplet and singlet components affect the conductance.

Specifically, we considered sp, df, and dp pairing states. The sp and df states produce ZBCPs whenever the triplet component is stronger than the singlet one. The peak is weaker in the case of df superconductors due to the anisotropic $d_{x^2-y^2}$ orbital form factor. In the strong-singlet limit, we found a dip structure in the conductance spectrum. For the sp state, in the regime where a finite, but small, triplet component coexists with a large singlet component, we predicted a weak ZBCP on top of the dip structure. This ZBCP disappears quickly with the decreasing triplet strength. For the df state, the weak ZBCP disappears rapidly already when the triplet component becomes smaller than the singlet component. In contrast, we found a ZBCP splitting for the dp state, which happens because the triplet component does not cause a sign change in the incoming and outgoing gaps. Thus, we conclude that making interfaces with different crystallographic orientations of the superconductor will be useful for drawing concrete conclusions in systems, where anisotropic orbital form factors are likely to be present.

In the context of the recent experimental results for CoSi$_2$/TiSi$_2$ heterostructures [18], we believe that the sp state is consistent with the experiments. We have performed our calculations for device sizes that are comparable to the experimental setup. We found that in the triplet-dominant regime, the opposite-chirality superconductivity on the two helical bands gives a ZBCP in the conductance of the T junction. This peak is quite robust and stronger than the

peak expected for the usual chiral p-wave superconductor [17]. Therefore, we think that the CoSi$_2$/TiSi$_2$ heterostructure is a triplet-dominant ($\Delta_{\text{singlet}} < \Delta_{\text{triplet}}$) superconductor. The conductance for an SN junction composed of such a triplet-dominant mixed-parity sp superconductor and a normal metal junction was studied earlier [24] and agrees with the CoSi$_2$/TiSi$_2$ tunnel junction data, barring the sharp feature at zero energy.

One of the major issues with our description of the CoSi$_2$/TiSi$_2$ heterostructures is the lack of the time-reversal symmetry breaking (TRSB) that has been observed up to T_c. The TRSB in the mixed-parity superconductors was predicted earlier [48,49]; however, it is expected to happen at a lower temperature below T_c. Twin boundaries can also cause TRSB, if the triplet and singlet components are comparable in magnitude [50]. Another possible explanation for the hysteresis observed in the magnetoresistance data is the Zeeman field induced supercurrent. In a superconductor with broken inversion symmetry, an in-plane Zeeman field gives rise to a supercurrent flow along the direction perpendicular to it [51,52]. We think that μSR experiments on CoSi$_2$/TiSi$_2$ heterostructures will provide ubiquitous evidence of TRSB.

We have considered a simple one-band model for CoSi$_2$ to qualitatively understand CoSi$_2$/TiSi$_2$ heterostructures. However, it is a multiband system, which could be a possible origin of the TRSB. We leave this issue of TRSB for future study. We conclude that the CoSi$_2$/TiSi$_2$ heterostructure is a $s + p$ mixed-parity superconducting state with a dominant p-wave component. Such a mixed-parity superconductor with a dominant triplet component is a topologically nontrivial system and is similar to a quantum spin Hall system [53,54]. It hosts topologically protected Andreev bound states, which carry spin currents, therefore constituting an important platform for further research.

ACKNOWLEDGMENTS

[1] N. Read and D. Green, Phys. Rev. B **61**, 10267 (2000).

[2] A. Y. Kitaev, Phys. Usp. **44**, 131 (2001).

[3] D. A. Ivanov, Phys. Rev. Lett. **86**, 268 (2001).

[4] A. Kitaev, Ann. Phys. (NY) **303**, 2 (2003).

[5] F. Wilczek, Nat. Phys. **5**, 614 (2009).

[6] C. Nayak, S. H. Simon, A. Stern, M. Freedman, and S. Das Sarma, Rev. Mod. Phys. **80**, 1083 (2008).

[7] R. M. Lutchyn, J. D. Sau, and S. Das Sarma, Phys. Rev. Lett. **105**, 077001 (2010).

[8] Y. Oreg, G. Refael, and F. von Oppen, Phys. Rev. Lett. **105**, 177002 (2010).

[9] V. Mourik, K. Zuo, S. M. Frolov, S. R. Plissard, E. P. A. M. Bakkers, and L. P. Kouwenhoven, Science **336**, 1003 (2012).

[10] S. Nadj-Perge, I. K. Drozdov, J. Li, H. Chen, S. Jeon, J. Seo, A. H. MacDonald, B. A. Bernevig, and A. Yazdani, Science **346**, 602 (2014).

[11] G. E. Volovik, *The Universe in a Helium Droplet* (Oxford University Press, Oxford, 2003).

[12] D. Wang, L. Kong, P. Fan, H. Chen, S. Zhu, W. Liu, L. Cao, Y. Sun, S. Du, J. Schneeloch, R. Zhong, G. Gu, L. Fu, H. Ding, and H.-J. Gao, Science **362**, 333 (2018).

[13] Q. Liu, C. Chen, T. Zhang, R. Peng, Y.-J. Yan, C.-H.-P. Wen, X. Lou, Y.-L. Huang, J.-P. Tian, X.-L. Dong, G.-W. Wang, W.-C.

Bao, Q.-H. Wang, Z.-P. Yin, Z.-X. Zhao, and D.-L. Feng, Phys. Rev. X **8**, 041056 (2018).

[14] L. Fu and C. L. Kane, Phys. Rev. Lett. **100**, 096407 (2008).

[15] H.-H. Sun, K.-W. Zhang, L.-H. Hu, C. Li, G.-Y. Wang, H.-Y. Ma, Z.-A. Xu, C.-L. Gao, D.-D. Guan, Y.-Y. Li, C. Liu, D. Qian, Y. Zhou, L. Fu, S.-C. Li, F.-C. Zhang, and J.-F. Jia, Phys. Rev. Lett. **116**, 257003 (2016).

[16] A. P. Mackenzie and Y. Maeno, Rev. Mod. Phys. **75**, 657 (2003).

[17] Y. Asano, Y. Tanaka, A. A. Golubov, and S. Kashiwaya, Phys. Rev. Lett. **99**, 067005 (2007).

[18] S.-P. Chiu, C. C. Tsuei, S.-S. Yeh, F.-C. Zhang, S. Kirchner, and J.-J. Lin, arXiv:2012.13679.

[19] G. E. Blonder, M. Tinkham, and T. M. Klapwijk, Phys. Rev. B **25**, 4515 (1982).

[20] B. T. Matthias, Phys. Rev. **87**, 380 (1952).

[21] L. F. Mattheiss and D. R. Hamann, Phys. Rev. B **37**, 10623 (1988).

[22] K. Tsutsumi, S. Takayanagi, and T. Hirano, Phys. B (Amsterdam, Neth.) **237–238**, 310 (1997).

[23] L. P. Gor'kov and E. I. Rashba, Phys. Rev. Lett. **87**, 037004 (2001).

[24] C. Iniotakis, N. Hayashi, Y. Sawa, T. Yokoyama, U. May, Y. Tanaka, and M. Sigrist, Phys. Rev. B **76**, 012501 (2007).

[25] A. B. Vorontsov, I. Vekhter, and M. Eschrig, Phys. Rev. Lett. **101**, 127003 (2008).

[26] Y. Tanaka, Y. Mizuno, T. Yokoyama, K. Yada, and M. Sato, Phys. Rev. Lett. **105**, 097002 (2010).

[27] M. Eschrig, C. Iniotakis, and Y. Tanaka, in *Noncentrosymmetric Superconductors*, edited by E. Bauer and M. Sigrist, Lecture Notes in Physics Vol. 847 (Springer, Berlin, 2012), pp. 313–357.

[28] S. Tamura and Y. Tanaka, Phys. Rev. B **99**, 184501 (2019).

[29] Y. Tada, N. Kawakami, and S. Fujimoto, J. Phys. Soc. Jpn. **77**, 054707 (2008).

[30] Y. Yanase and M. Sigrist, J. Phys. Soc. Jpn. **77**, 124711 (2008).

[31] K. D. Usadel, Phys. Rev. Lett. **25**, 507 (1970).

[32] N. Hayashi, K. Wakabayashi, P. A. Frigeri, and M. Sigrist, Phys. Rev. B **73**, 092508 (2006).

[33] P. A. Frigeri, D. F. Agterberg, A. Koga, and M. Sigrist, Phys. Rev. Lett. **92**, 097001 (2004); P. A. Frigeri, D. F. Agterberg, I. Milat, and M. Sigrist, arXiv:cond-mat/0505108.

[34] V. P. Mineev and K. V. Samokhin, Phys. Rev. B **78**, 144503 (2008).

[35] G. Annunziata, D. Manske, and J. Linder, Phys. Rev. B **86**, 174514 (2012).

[36] A. Zaitsev, Phys. Lett. A **194**, 315 (1994).

[37] Y. V. Nazarov, Superlattices Microstruct. **25**, 1221 (1999).

[38] Y. Tanaka, Y. V. Nazarov, and S. Kashiwaya, Phys. Rev. Lett. **90**, 167003 (2003).

[39] Y. Tanaka, Y. V. Nazarov, A. A. Golubov, and S. Kashiwaya, Phys. Rev. B **69**, 144519 (2004); **70**, 219907(E) (2004).

[40] Y. Tanaka and S. Kashiwaya, Phys. Rev. B **70**, 012507 (2004).

[41] Y. Tanaka, Y. Asano, A. A. Golubov, and S. Kashiwaya, Phys. Rev. B **72**, 140503(R) (2005); **73**, 059901(E) (2006).

[42] Y. Tanaka, S. Kashiwaya, and T. Yokoyama, Phys. Rev. B **71**, 094513 (2005).

[43] J. P. Morten, A. Brataas, and W. Belzig, Phys. Rev. B **72**, 014510 (2005).

[44] Y. Tanaka and A. A. Golubov, Phys. Rev. Lett. **98**, 037003 (2007).

[45] Y. Tanaka, M. Sato, and N. Nagaosa, J. Phys. Soc. Jpn. **81**, 011013 (2012).

[46] A. F. Volkov and H. Takayanagi, Phys. Rev. Lett. **76**, 4026 (1996); Phys. Rev. B **56**, 11184 (1997).

[47] Y. Asano, Phys. Rev. B **64**, 014511 (2001).

[48] C. Timm, S. Rex, and P. M. R. Brydon, Phys. Rev. B **91**, 180503(R) (2015).

[49] Y. Wang and L. Fu, Phys. Rev. Lett. **119**, 187003 (2017).

[50] E. Arahata, T. Neupert, and M. Sigrist, Phys. Rev. B **87**, 220504(R) (2013).

[51] S. K. Yip, Phys. Rev. B **65**, 144508 (2002).

[52] V. M. Edelstein, Phys. Rev. B **67**, 020505(R) (2003).

[53] Y. Tanaka, T. Yokoyama, A. V. Balatsky, and N. Nagaosa, Phys. Rev. B **79**, 060505(R) (2009).

[54] M. Sato and S. Fujimoto, Phys. Rev. B **79**, 094504 (2009).